

Periodic Intensity Fluctuations of Balmer Lines from Single-Foil Excited Fast Hydrogen Atoms*

I. A. Sellin, C. D. Moak, P. M. Griffin, and J. A. Biggerstaff

Oak Ridge National Laboratory, Oak Ridge, Tennessee 37830

(Received 2 April 1969)

Protons with velocities ranging from 3.2×10^8 to 6.3×10^8 cm/sec were passed through a carbon foil producing excited hydrogen atoms which decayed in flight after emergence. With the foil in magnetic fields from 2 to 25 G, the lines H_α through H_ϵ showed periodic intensity fluctuations due to Stark mixings of fine-structure levels caused by motional electric fields (6–158 V/cm). An extension of the Bethe-Lamb theory of Stark quenching provides good agreement between a small number of theoretically dominant frequencies and the measured fluctuation frequencies. Apparent discrepancies between theory and experiment noted by other experimenters are shown to be removed by our calculations except in one measurement on Ly_α . The necessity of using double foils postulated in the previous work is discussed. Our analysis suggests the preferential alignment of the final-state angular momenta perpendicular to the beam direction. Reasons for this alignment are given.

INTRODUCTION

Periodic intensity fluctuations of spectral lines from fast hydrogen atoms emerging in a given quantum state n after passage through foils were first experimentally observed by Bashkin *et al.*¹ These intensity fluctuations can be attributed to Stark mixing of fine-structure (fs) levels decaying with very different line intensities, with the result that weakly radiating levels can periodically "feed" a strongly radiating level giving rise to short bursts of light. Directly pertinent theoretical discussions of related phenomena have been given by Lamb,² Series,³ and Wangsness.⁴

At the time of the earliest experiments, only molecular ions of hydrogen seemed to produce the effect which occurred on some but not all observed lines, and it was necessary to use two foils to cause the beam to show intensity fluctuations. In our work, intensity fluctuations are seen with incident atomic ions on every line we have observed, and double foil techniques are unnecessary. We explain the difference between the two experiments as follows: When a molecular beam passes through a foil and produces a H^0 atom, the remainder of the original molecule is still nearby, most probably as a H^+ ion. This ion produces a field at the atom comparable to the externally applied fields used in these experiments (~ 10 V/cm) until the particles have become separated by about 10^{-4} cm. During this time, due to the initially very high field, a very large number of intensity fluctuations will have taken place, the exact number depending on the relative trajectories of the two fragments. We show later that the fluctuation frequency is approximately proportional to the electric field strength. The end res-

ult is that the fluctuations have acquired an essentially random phase, due to the differing microscopic trajectories of the various pairs of particles, by the time our macroscopic measurement begins. However, since the dissociation products achieve "independence," taken to mean separation greater than 10^{-4} cm, in about 10^{-2} cm of forward travel at 100 keV/ion, a second foil placed at this or greater distance from the first results in a reexcitation of the independent fragments (essentially 100% of the beam will be dissociated in the first foil). Since mounting foils closer together than 10^{-2} cm is not practical, the results of a "molecular beam plus two foils" experiment and an "atomic beam plus single foil" experiment should be the same.

In our apparatus, protons with velocities ranging from 3.2×10^8 to 6.3×10^8 cm/sec passing through carbon foils of 5–20 $\mu\text{g}/\text{cm}^2$ thickness in a magnetic field of 2–25 G (or alternatively in electrostatic fields of strength 6–158 V/cm) produced a stream of radiating atoms which exhibited the now-familiar "dotted-line" traces of light emitted as the atoms moved downstream from the foil.

Several interesting features of these flashes of light immediately suggest themselves. Clearly, the atoms are created in times no greater than the transit time of the particle through the foil, times of order 10^{-14} sec. Distance along the flight path from the foil can be translated into time delay following creation of the atom. Whatever mechanisms operate to cause the atom to alternately emit and not emit light as it proceeds along its path must not only operate for all atoms created in the foil but must operate always with the same relative phase for every atom created. Otherwise one atom would emit light at places

where another atom would be quiescent and all evidence of light-intensity fluctuations would be obliterated in a photographic integration. It would appear that the wave function describing a suitable superposition of fs Stark-mixed levels, while perhaps having random phases among the constituent states, must at time zero (at the foil) have definite average values for the population probabilities of the various constituent states. A relevant observation is that, within experimental error, the first maximum in the fluctuation pattern occurs at the foil, indicating a high initial population of the strongly radiating fs states relative to others which are subsequently fed by them. Why this should be true seems to involve model-dependent dynamical assumptions about the collision process. Such physical constraints certainly would not be contained in the general set of Stark-coupled wave equations which would be constructed for an otherwise isolated atom in an arbitrary excited state, since any set of initial relative amplitudes and phases would be mathematically acceptable. Specific dynamical boundary conditions would have to be applied to establish the initial populations of the states in the mixture. Fortunately, much information can be obtained by studying the frequencies alone. When application of boundary conditions becomes necessary, the assumed conditions turn out to be reasonable and not unduly restrictive.

Theoretical examination of the level structure of hydrogen in the presence of perturbing electric fields indicates the possibility of a very large number of fluctuation frequency components which could occur. Some of these are observed, but close examination is required in order to understand why certain possible fluctuation frequencies

among those observable by the present techniques do not appear. Small radiative decay probabilities should be responsible for failure to observe certain flicker rates since one or more states would have excessively slow light emission. The simplicity of the light fluctuation patterns for the large number of remaining cases requires some additional reasonable physical assumptions for its explanation as discussed below. Evidence for alignment of final-state angular momenta perpendicular to the beam direction can be inferred from this simplicity as well as from the actual frequency measurements.

EXPERIMENTAL ARRANGEMENT

As shown in Fig. 1, protons from a 0–200-keV accelerator were collimated into a 3.2-mm-diam beam which passed through the carbon foil, through a glass target chamber (9-cm diam, 72-cm length), and were finally stopped in a Faraday cup. Protons of energy 50, 100, and 200 keV were used in these experiments. The final 3.2-mm collimator was 30 cm from the carbon foil. The chamber inner wall was coated with graphite except for two 1.5-cm-wide strips which served as viewing ports. The coatings were held at ground potential to avoid unwanted electrostatic fields. Iron plates above and below the glass chamber were used with various permanent magnet configurations to produce magnetic fields in the range 2–25 G. For viewing along the magnetic field, a 45° strip mirror was placed below the beam and its light was fed out through a second slot in the graphite coating. A 4×5-in. f/4.5 camera was mounted 120 cm from the beam axis at right angles to the target chamber, and the entire apparatus was sur-

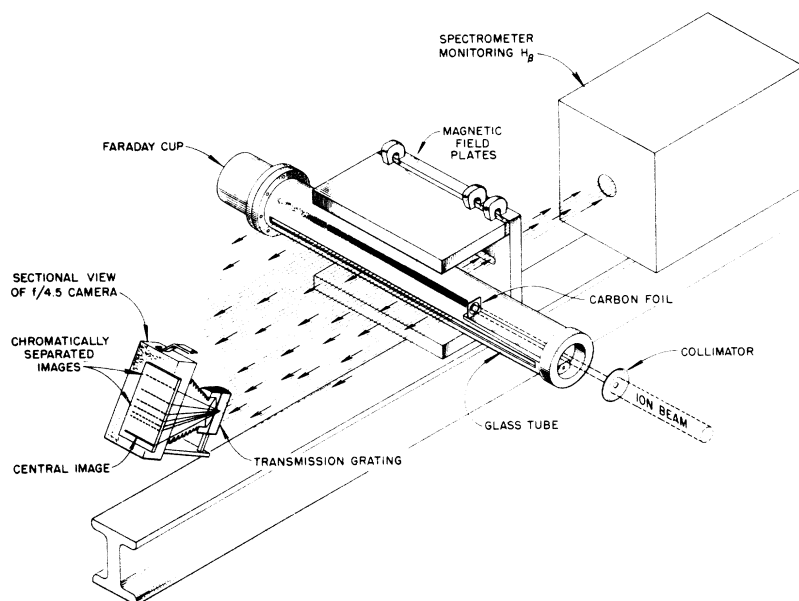


FIG. 1. Schematic diagram of the apparatus.

rounded by a light tight box. A 600-lines/mm transmission grating with a 32×32 -mm ruled area was mounted on the camera lens with grooves parallel to the beam. With this arrangement monochromatic images of the beam were separated on the photographic plate. The camera was pointed somewhat below the plane of the beam so that the undiffracted image fell near the bottom of the photographic plate and the spectrum images fell near the middle of the plate and near the camera lens axis. The system had an effective reciprocal dispersion of about $100 \text{ \AA}/\text{mm}$. Monochromatic images on the plate were about $400 \mu\text{m}$ wide and 2 cm long. The magnification of the optical system was measured in order to establish the relationship between distances on the photographic plate and distances along the beam. Eastman Kodak 103a-O and 103a-F plates were used throughout and exposure times ranged from 30 min to 6 h. All the measurements were based on densitometer traces of the monochromatic beam images using a modified Knorr-Albers microphotometer.

DISCUSSION AND RESULTS

We assume that the wave function for a hydrogen atom emerging with principal quantum number n from a foil located within a weak electric field F can be described in terms of a coherent mixture of the fs levels. Sudden excitation conditions are appropriate, since the particle transit time through the foil is $\leq 10^{-14}$ sec, whereas, the inverse fs splittings are $\geq 10^{-9}$ sec. The Stark matrix elements couple the levels pairwise according to the rules $\Delta L = 1$ and $\Delta m_j = 0$. It is well known that in the simplest case of a weakly damped two-level system, oscillations of the amplitudes (a_1 , a_2) of the two-coupled states occur. This leads to terms in the occupation probability of each state which oscillate at a frequency corresponding to the perturbed energy separation of the two levels.^{5, 6} In the three-level case there are terms in the occupation probability of each state which oscillate at each of the three possible level separation⁶ frequencies. In the general multilevel case, there will occur many oscillatory terms in the occupation probability of each state, one corresponding to each perturbed level separation frequency. The total number of such terms is

$$\sum_{\text{all } |m_j|} \frac{1}{2}(2n - 2|m_j| - 1)(2n - 2|m_j|).$$

Since, in general, all of the levels are radiatively damped, the same frequencies are expected to modulate the downward transition probabilities for spectral lines originating from these levels. Although the number of conceivable frequencies is large (for example, 36 for the $n = 5$, $m_j = \frac{1}{2}$ case

along), we have found it possible to achieve good agreement between measured frequencies and a very few calculated frequencies which we show to be dominant on plausible grounds.

The usual time-independent perturbation theory of the weak-field Stark effect is first used to approximately calculate the perturbed energy and eigenfunction of each level in a given fs multiplet. We thus neglect quadratic or higher terms in F and the effects of radiative widths on the level energies, as in the treatments of Lüders⁷ and of Bethe and Salpeter.⁸ The level-structure calculations are patterned after the similar ones of Lüders, where details we omit may be found. The $|njm_j\rangle$ representation is used for the unperturbed eigenfunctions, so that the fs perturbation terms appear along the diagonal of the symmetric perturbation matrix

$$H' \equiv H_{\text{fs}} + H_{\text{rad}} + H_{\text{Stark}} \quad (1)$$

The quantity H_{rad} (omitted by Lüders) is the radiative level shift for each fs level and is included phenomenologically by adding its numerical value⁹ to the corresponding diagonal term. Inclusion of these shifts is rather unimportant except for the s-like levels where the shift is comparable to the fs splittings. The diagonal terms of H' are thus of the form

$$H_{\text{fs}} + H_{\text{rad}} = (Z^4 \alpha^2 Ry / 4n^4) [3 - 4n / (j + \frac{1}{2})] + \Delta(njl), \quad (2)$$

where Δ represents the radiative shift and the other symbols have their conventional meanings. The (11) element corresponds to $j = n - \frac{1}{2}$, $l = n - 1$; the (22) to $j = n - \frac{3}{2}$, $l = n - 1$; the (33) to $j = n - \frac{5}{2}$, $l = n - 2$, etc. The symmetric Stark matrix elements in the form given by Lüders are displayed on the diagonals once and twice removed from the main diagonal (once if $\Delta j = 0$ and twice if $\Delta j = 1$). The perturbation matrix is then diagonalized and eigenfunctions calculated.

An example of the level structure resulting from this diagonalization procedure is given as a function of F in Fig. 2, for the case $n = 5$, $m_j = \frac{1}{2}$, $\frac{3}{2}$, $\frac{5}{2}$. The normalized eigenvector corresponding to each perturbed-term value is obtained as a specific linear combination of the unperturbed states. Table I presents the numerical coefficients for this same case at a field strength of 70 V/cm. Inversion of the eigenvector matrix yields each $|njm_j\rangle$ state as a linear combination of the new eigenstates, which can be regarded as normal modes of the system when their time dependence is included.

Once the level terms and eigenfunctions are

TABLE I. Perturbed terms and eigenvectors corresponding to the terms for $n=5$, $m_j = \frac{5}{2}$, at 70 V/cm.

Term value (MHz) ^a	Eigenvector components				
	$g_{9/2}$	$g_{7/2}$	$f_{7/2}$	$f_{5/2}$	$d_{5/2}$
1247	-0.4492	0.2077	-0.6689	0.2364	-0.5017
561	-0.3408	-0.6527	-0.2281	-0.6358	0.0395
-89	0.6656	-0.3559	-0.0706	-0.0065	-0.6522
-785	0.3220	0.5939	-0.3020	-0.6712	0.0440
-1447	0.3680	-0.2269	-0.6359	0.2990	0.5652

^aZero of energy corresponds to the energy of the highest j state at zero field.

established, the harmonic content of the Balmer radiation from specific superpositions of the levels can be studied. As will be discussed in detail, the magnitude of each coefficient in the linear combination of normal modes contributing to each strongly radiating $|njm_j\rangle$ state markedly influences the relative importance of each possible frequency component. Favorable comparison between our model and experiment is obtained for just those few frequencies which turn out to be dominant on theoretical grounds.

Some essential differences exist between our approach and the similar but more approximate approach of Wangness as applied by Bickel and Bashkin.¹ They have taken into account the linear Stark splittings which result from coupling only two adjacent levels in the perturbation matrix. As Fig. 2 shows, curvature and repulsion of levels are pronounced at the fields used in most of our experiments as well as in theirs. We believe that this inadequate approximation is the fundamental reason for the apparent discrepancies between theory and experiment. As we will show, the application of our model to their measurements

accounts qualitatively for their published observations as well, save in the case of the Ly_α measurement made by Bickel.¹⁰ There remains a serious disagreement in this one case alone. (See note added in proof.)

Let us now consider the reason for the reduction of the rich spectrum of possible frequency components in the emitted light to the small number suggested by observation. We list several considerations which aid in interpreting the results of the more complete calculations which follow. In an unperturbed fs multiplet contributing to the intensity of a given Balmer series line, the transitions arising from upper d levels are considerably stronger than any others. These are the highest orbital angular momentum states allowed in Balmer radiation, and have downward transition probabilities about twice that of their nearest competitors, the p levels. Their large multiplicity reinforces this dominance.

Empirically we found that a large number of possible frequencies would not appear and remarkably good agreement between calculated and measured frequencies could be brought about by considering only the highest magnetic substates allowed in the Balmer series, $m_j = \frac{5}{2}, \frac{3}{2}$ corresponding to $m_l = 2$. As a result, some very recent pertinent calculations of Mapleton¹¹ on fast binary electron capture processes were sought out. His work shows that, for at least a few well-defined cases so far studied, population of high m_l substates predominates by an order of magnitude over capture into states $m_l \sim 0$, where the axis of quantization is taken in a plane perpendicular to the beam direction. Classically, the conditions of each proton passage through the foil are such that the average angular momentum of all foil electrons relative to the proton lies in a plane perpendicular to the beam direction. Schematically it is as though there were a reservoir of electrons with angular momentum in the plane which feeds this favored alignment to the final collision products. In Mapleton's paper, m_l rather than m_j is the natural quantity to use, because the spin-orbit precession times are all much longer than atomic collision times. Through inspection of the

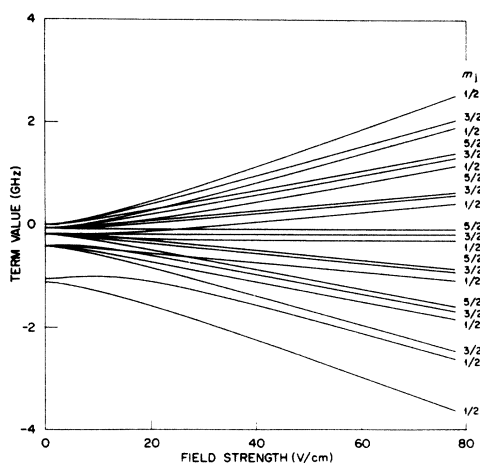
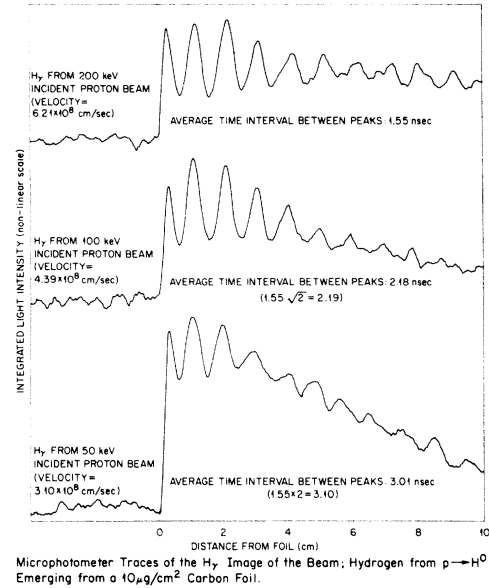


FIG. 2. Sample calculated level structure for $n=5$, $m_j = \frac{1}{2}, \frac{3}{2}, \frac{5}{2}$, as a function of electric field.

appropriate Clebsch-Gordon coefficients, it can be seen that substates of given m_l are apportioned equally among the classifications $m_j = m_l + \frac{1}{2}$ and $m_j = m_l - \frac{1}{2}$. If it is assumed that for a foil target and for given l only the states of highest m_l are substantially populated, then the substate $m_j = m_l + \frac{1}{2}$ corresponds wholly to $j = l + \frac{1}{2}$. The substate $m_j = m_l - \frac{1}{2}$ is partitioned between the two states $j = l + \frac{1}{2}$ and $j = l - \frac{1}{2}$ (mostly the latter), which are split by the spin-orbit and Stark interactions. Thus, of the two possibilities for m_j , the $m_j = m_l + \frac{1}{2}$ case is slightly less "diluted."

For the above reasons, we argue that favorable comparisons between theoretical and observed frequencies in Balmer lines are likely to result from scrutiny of the perturbed level structure for m_j equal to either $\frac{5}{2}$ or $\frac{3}{2}$. We show that heavier weighting of the $m_j = \frac{1}{2}$ states markedly enhances the harmonic content of the light emitted, in contrast with the simplicity of the data.

The alignment implied by preferential population of states of high m_j is evident. It may be that states having $m_j > \frac{5}{2}$ are even more strongly populated, but Balmer transitions from these states are forbidden even in an electric field. It might be thought that the magnetic field providing the motional electric field would alter this situation, but since $\mu_B B$ for this experiment is only $\leq 10^7 \text{ sec}^{-1}$, the electric field effects are much the stronger. The use of a motional electric field is responsible for an effect which serves as a check on attribution of the fluctuation effects to Stark mixing of fs levels. When the beam velocity was varied by as much as a factor of 2, the locations of intensity maxima were approximately fixed in space. If the fluctuation frequencies were fixed, the spatial pattern would instead be stretched in proportion to the beam velocity. At the fields used, however, some of the Stark splittings are still approximately linear with the motional field, which is in turn linear with the beam velocity. Thus, the ratio of term splitting to beam velocity is invariant to the extent that the Stark splittings are linear. This is exactly what is required for space-fixed intensity maxima. An illustration of this effect is shown in Fig. 3. Of course, any case for which the relevant Stark splittings are appreciably nonlinear will not conform to this rule. Further insight into the important frequency components results from consideration of just which perturbed eigenstates are important in constructing a "d-like" initial state, that is, a state which will radiate a Balmer line strongly. It was noted in the earlier discussion of Table I that inversion of the eigenvector matrix provides an expansion of each original eigenfunction in terms of the perturbed eigenfunctions. Since H' is symmetric, the inverse matrix is the transpose of the tabulated one, and one can assess the importance of each of the perturbed eigenfunctions by the size



Microphotometer Traces of the H_γ Image of the Beam; Hydrogen from $p \rightarrow H^0$ Emerging from a $10 \mu\text{g}/\text{cm}^2$ Carbon Foil.

FIG. 3. Traces showing approximate invariance of spatial separation of intensity maxima with beam velocity.

of its coefficient in the columns labeled $d_{5/2}$ and $d_{3/2}$. As in Lamb's treatment,⁶ we consider each state amplitude a_i to be expressible as a sum over appropriate constants times the corresponding time dependences

$$a_i = \sum_k A_k \exp[(-\mu_k + i\omega_i)t], \quad (3)$$

$$\text{where } \psi = \sum_i a_i u_i \exp(-i\omega_i t). \quad (4)$$

In this expression, a_i is the amplitude of an unperturbed atomic eigenstate such as $d_{5/2}^{3/2}$ or $d_{3/2}^{3/2}$ (the superscript denotes m_j); A_k is an arbitrary constant which depends implicitly upon the relative importance of the k th perturbed eigenstate in constructing a_i as well as explicitly upon initial conditions; ω_i is the unperturbed energy of level i in frequency units; μ_k is the complex number corresponding to the energy of the k th perturbed eigenstate. A similar but distinct set of such equations is used for each value of m_j , a good quantum number. The imaginary part of μ_k is just 2π times a perturbed-term value like those shown in Table I (neglecting radiative width effects on level energies as before). The real part of μ_k is half the corresponding radiative width of mode k . Its value is close to half the unperturbed decay probability of the corresponding pure state at small electric fields and approaches an average characteristic of all of the levels at sufficiently large fields. Since our entire experiment is over in times comparable to one e -folding time of the shortest-lived level in the mix, we neglect the real part of μ_k compared to the imaginary part of

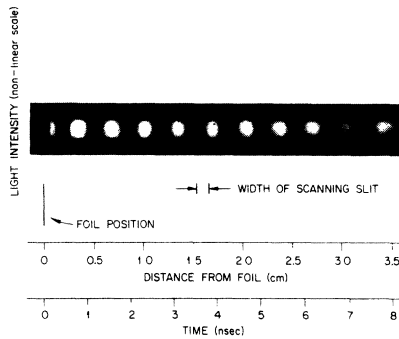


FIG. 4. Sample photograph and densitometer trace for H_γ line intensity at a field of 70 V/cm.

μ_k in investigating the periodic behavior of the population probabilities $|a_i|^2$. In so doing we give up our knowledge of the time decay of the envelope of the oscillations corresponding to the falloff of line intensity displayed in the photographic traces as in Fig. 4.¹² The harmonic behavior of a_i is not altered by neglecting the real part of μ_k , since functions of the type $\exp[(-\frac{1}{2}\gamma' - i\omega'_k)t]$ have phase-shifted maxima and minima occurring with frequency ω'_k (the primes denote perturbed quantities).

The wave function may be calculated directly from Eq. (4). The sum over i goes over all j and m_j for a given n . When the electric dipole matrix element is summed over the final $n=2$ states and squared, cross terms of the type

$$A_k^* A_j \exp[(-\mu_k^* - \mu_j)t] + c. c. \quad (5)$$

occur, one pair for each possible level separation frequency $i\omega'_{jk} \equiv \mu_k^* + \mu_j$. In the sum over final states, the $n=2$ levels are regarded as unperturbed, since the effect of fields ≤ 100 V/cm on the well separated $n=2$ levels is slight.

The dependence on initial conditions is contained in the constants A_k . Many choices could, of course, be made. A choice that matches well our experimental observations is as follows: The occupation probability $|a_i|^2$ at $t=0$ is assumed to have a certain mean value when averaged over all collisions, but the phase between a_i and a_j is assumed random from collision to collision. Assuming random phases allows one to calculate the total electric dipole transition probability by summing the separate occupation probabilities, weighted by their corresponding Balmer transition probabilities. Such assumptions about phase relationships are qualitatively unimportant so long as one avoids preferential excitations of pure normal modes, which, of course, do not beat with one another. For a capture into a given angular momentum state l , only the substate of highest m_l is assumed

populated, for the reasons discussed previously.

Captures into states of different l should be given a relative weight characteristic of high-energy collisions. We find that the choice of weights which best matches our experimental observations lies between a flat weighting with l (1 for $m_l=l$ and 0 for the other m_l values), and a weight of $2l+1$ for each l (reminiscent of shadow scattering in nuclear-reaction theory and not having to do with $2l+1$ possible values of m_l). This weighting is not at all critical, since either extreme provides a reasonable match to the data.

The result of using these initial conditions to calculate the square of the total dipole matrix element, and thus the relative line intensity as a function of time, is shown in the top trace of Fig. 5 for the case of H_γ at a field of 70 V/cm. This top trace is to be compared directly with the experimentally observed trace in Fig. 4. The other traces on Fig. 5 show the separate contributions to the total line intensity when the initial state is assumed to be an f , d , p , and s state, respectively. For these lower traces all the appropriate sums and weights have been included, except for the $2l+1$ weight used when these separate traces are summed to give the top trace. Except for the weight which the collision process assigns to each l state, the relative peak heights of these traces are a direct measure of the importance of each l state in contributing to the over-all line intensity. As expected, an initially pure f state contributes nothing to the total intensity at $t=0$; a pure d state radiates more strongly at $t=0$ than at later times, when it becomes mixed with states having smaller Balmer transition probabilities. The traces for p and s states are intermediate. The experimental observation that the total intensity is peaked at the foil means that a combination of large d -level transition probability and initial d -state population dominates the flicker pattern. The close agreement between the peak positions of the d -level

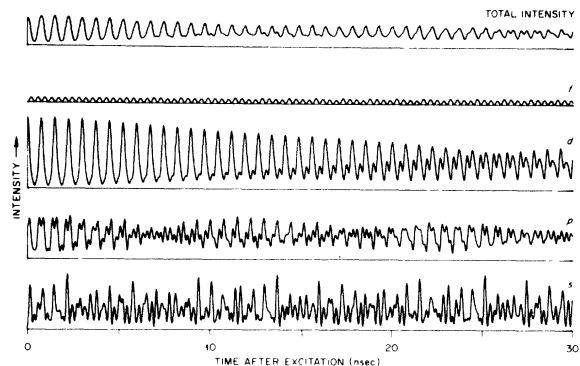


FIG. 5. Total intensity of the H_γ line as a function of time at 70 V/cm; components of the total intensity associated with each pure l state.

trace and of the top trace shows that the d levels determine the basic flicker rates, providing they are substantially populated in the collision process.

The d -level trace in Fig. 5 can be broken down into its constituents, some of which are plotted in Fig. 6. The top four traces on this plot display the population probability of the $nd_{5/2}^{5/2}$ level at 70 V/cm, assuming that initially the atom is in the $nd_{5/2}^{5/2}$ state. It is seen that the trace for $n=5$ is a near twin to the d -level trace in Fig. 5.

The bottom trace in Fig. 6 plots the occupation probability of a $5d_{5/2}^{1/2}$ state, assuming that the atom is in that pure state initially. This pattern is much more complex than for $m_j = \frac{5}{2}$ and clearly resembles the data far less closely. It has been generally true for the wide range of cases we have investigated that the over-all calculated intensity of a line shows simple flicker structure in agreement with our data when the states of highest m_l are included, and that the simple structure disappears when states of lower m_l are included. We interpret this as evidence for preferential population of states of high m_l , where the axis of quantization is perpendicular to the beam direction. Since our apparatus is polarization insensitive, and the flicker patterns are qualitatively similar when viewed parallel and perpendicular to the field direction, we have not yet attempted to investigate peculiarities in the angular distribution and polarization of the light implied by asymmetric m_l populations.

A direct comparison between the prominent flicker frequency components observed and those obtained from our calculated intensity plots is presented in Table II.¹² The agreement is good in every case. At the lower fields, the calculated

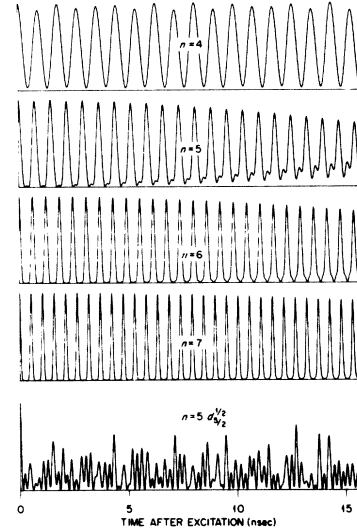


FIG. 6. Population probabilities of an initially pure $nd_{5/2}^{5/2}$ state as a function of time; population probability of an initially pure $5d_{5/2}^{1/2}$ state as a function of time. The field strength is 70 V/cm.

plots sometimes show two basic peak spacings, a feature of some of the observed data as well. Double entries in Table II refer to these cases.

The flicker patterns for $n=3$ deserve special comment. The flicker frequency for H_{α} was difficult to observe experimentally, because the apparent modulation of the total intensity was small and the pattern rather irregular. We note that for $n=3$, the $d_{5/2}^{5/2}$ level is pure and cannot beat with any other level. The analog of Fig. 5 for the case $n=3$ gives an over-all intensity which is weakly

TABLE II. Comparison of prominent flicker frequency components observed experimentally and calculated theoretically in this work.

Field strength (V/cm)	Direction of view relative to F	Line observed	Prominent observed frequencies (MHz)	Prominent calculated frequencies (MHz) at nominal field
70±7	⊥	H_{α}	790±40	792
70±7	∥	H_{α}	823±40	792
70±7	⊥	H_{β}	1035±50	1103±5
70±7	∥	H_{β}	1150±50	1103±5
70±7	⊥	H_{γ}	1360±40	1346±7
70±7	∥	H_{γ}	1350±40	1346±7
70±7	⊥	H_{δ}	1590±50	1612±8
12±1	⊥	H_{β}	320±15	306±2
12±1	∥	H_{β}	302±15	306±2
12±1	⊥	H_{γ}	301±15	272±2
12±1	∥	H_{γ}	258±15	258±2
12±1	⊥	H_{δ}	308±15	301±2
12±1	∥	H_{δ}	308±15	286±2
12±1	⊥	H_{ϵ}	349±20	335±2
12±1	∥	H_{ϵ}	349±20	323±2

modulated and not very regular, and has as one of its substantial frequency components the perturbed $s_{1/2} - p_{1/2}$ level splitting of 792 MHz, in agreement with the frequency observed. Thus, in the one case we have investigated in which our model does not yield a simple result, experimental observation yields a similarly obscure pattern containing one of the calculated frequency components.

Comparisons can be made to measurements of various University of Arizona experimenters on Ly_α in hydrogen¹⁰ and on various He^+ transitions¹ to which our calculations can easily be scaled. At the field strength of 120 V/cm used for the Ly_α case, the calculations predict that the oscillations should occur at a frequency higher by only a few percent than the Lamb shift frequency, 1058 MHz. The experimental result was 2200 ± 200 MHz. We do not understand this serious discrepancy and

TABLE III. Comparison of prominent flicker frequencies for He^+ observed by the authors of Ref. 1 with those calculated from the present method.

Comparison of calculated frequencies in experiments on He^+			
Field strength (V/cm)	Transition observed $n-n'$	Prominent observed frequency (MHz)	Prominent calculated frequency (MHz)
40	4-8	560	645
40	4-9	610	695
60	4-7	770	830
60	4-8	820	930
60	4-9	880	1035
60	4-10	950	1150

suggest that another experimental measurement be made.

Comparisons to the published He^+ data are considerably better. Table III shows the observed frequencies as well as a suitable average of the prominent calculated frequencies, which turned out to be close to one another. The scaling procedure amounts to reducing the field strength in hydrogen by an effective factor of Z^5 and then amplifying the resulting level structure by a factor of Z^4 . The m_j dependence of the calculated fluctuation frequencies was very slight. The magnitudes are in better agreement with the measured results than the two-level calculations of the experimenters. An increase of a few percent in the assumed field strength would materially improve the agreement. More significant is that the trend of the frequencies with both n and with field strength is correctly reproduced, a feature which was not provided by the two-level calculations of the earlier experimenters.

Note added in proof. We have performed the suggested Ly_α experiments, at motional electric fields of 197 V/cm and 118 V/cm; the results, 1340 and 1220 MHz, respectively, are both in agreement with our calculations (to well within the $\pm 5\%$ experimental error limits) and in disagreement with the results of Bickel.¹⁰

ACKNOWLEDGEMENT

We are grateful to G. K. Werner of this Laboratory for his many helpful suggestions and assistance in the design of the experimental facilities and in the reduction of the data.

*Research sponsored by the U. S. Atomic Energy Commission under contract with Union Carbide Corporation.

¹S. Bashkin, W. S. Bickel, D. Fink, and R. K. Wangsness, Phys. Rev. Letters **15**, 284 (1965); W. S. Bickel and S. Bashkin, Phys. Rev. **162**, 12 (1967).

²W. E. Lamb, Jr., Phys. Rev. **85**, 259 (1952).

³G. W. Series, Phys. Rev. **136**, A684 (1964).

⁴R. K. Wangsness, Phys. Rev. **149**, 60 (1966).

⁵H. A. Bethe and E. E. Salpeter, Quantum Mechanics of One- and Two-Electron Atoms (Academic Press Inc.,

New York, 1957), p. 290.

⁶See Ref. 2, p. 272.

⁷G. Lüders, Ann. Physik **8**, 20 (1951).

⁸See Ref. 5, p. 286.

⁹See Ref. 5, p. 103.

¹⁰W. S. Bickel, J. Opt. Soc. Am. **58**, 219 (1968).

¹¹R. A. Mapleton, J. Phys. **B1**, 850 (1968).

¹²Only qualitative comparisons could be made because of the nonlinear intensity response of the photographic plates.

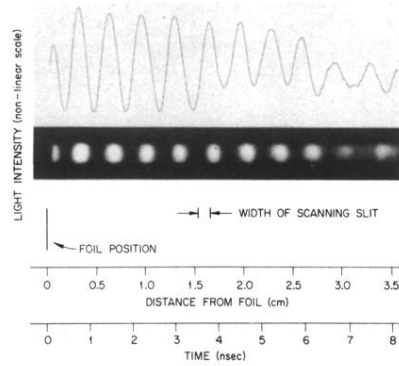


FIG. 4. Sample photograph and densitometer trace for H_{γ} line intensity at a field of 70 V/cm.